2.5

FROM CLOUD ORGANIZATION TO CLIMATE SENSITIVITY -- THE CLOUD OBJECT APPROACH

Kuan-Man Xu*, Bruce A. Wielicki, and Takmeng Wong

NASA Langley Research Center, Hampton, VA

1. INTRODUCTION

It is well known that clouds are organized into systems such as mesoscale convective complexes and squall lines. In the tropics and summertime midlatitudes, these systems are known for creating violent weather. Because these systems are characterized not only by their large horizontal extent but also for their long duration, they can also impact climate. On the other hand, subtropical boundary-layer cloud systems are the persistent weather phenomena off the west coasts of the continents and they are known to play important roles in climate and climate sensitivity. All of these cloud systems are strongly controlled by or associated with large-scale dynamical structures or circulations. Thus, weather and climate are ultimately linked through large-scale circulations.

The cloud object approach identifies a cloud object as a contiguous patch of the Earth composed of satellite footprints within a single dominant cloud-system type (Xu et al. 2005). The shape and size of a cloud object are determined by the satellite footprint data and by the selection criteria based upon cloud physical properties for a given cloud-system type. The selection criteria determine what types of cloud systems will be identified from satellite footprint data. For example, the selection criteria for tropical deep convective cloud objects are composed of requirements for cloud top height, cloud optical depth and footprint cloud fraction while boundary-layer cloud object types are determined by footprint cloud fraction and cloud top height.

Individual cloud objects are a collection of weather phenomena. They are "snapshots" of cloud systems along a satellite swath because the satellite scanning time is only a few minutes. Their physical properties differ greatly from one cloud object to another because of the short-term variabilities of the dynamical structures. These variations thus represent "weather noises," rather than long-term climatic signals. In order to study climate and climate sensitivity using the cloud object data, large ensembles of cloud objects categorized by the matched atmospheric states or specific climate conditions should be combined to generate statistically robust cloud-physical characteristics. These characteristics are analyzed in terms of the summary probability density functions (pdfs) or histograms over an ensemble of cloud objects, i.e., the combined pdfs of individual cloud objects, instead of simple averages and standard deviations.

Two sets of cloud-object analyses will be presented in this study. The tropical deep convective cloud object data are analyzed to provide supporting evidence for the fixed anvil temperature hypothesis of Hartmann and Larson (2002). It is found that the changes in macrophysical properties of cloud objects over the entire tropical Pacific were small for the large-size category of cloud objects, relative to those of the small- and medium-size categories (Xu et al. 2006a). Another set of analyses contrasts the statistical characteristics of boundary-layer cloud object types between the tropics and the subtropics (Xu et al. 2006b). It is found that each of the three boundary-layer cloud object types (cumulus, stratocumulus and stratus) exhibits small differences in statistical distributions of cloud optical depth, liquid water path, TOA albedo and cloud-top height, but large differences in those of cloud-top temperature and OLR between the tropical and subtropical Pacific regions. These results can be explained by the differences in the sea surface temperature (SST) distributions and the (local) boundary-layer dynamics.

2. THE CLOUD OBJECT APPROACH

A cloud object is defined as a contiguous patch composed of Clouds and the Earth's Radiant Energy System (CERES; Wielicki et al. 1996) footprints that satisfy a set of physically-based cloud-system selection criteria. A "region-growing" strategy based on imager-derived cloud properties is used to identify the cloud objects within a single

*Corresponding author's address: Dr. Kuan-Man Xu, Mail Stop 420, NASA Langley Research Center, Hampton, VA 23681; Email: Kuan-Man.Xu@nasa.gov.

satellite swath (Wielicki and Welch 1986). For all CERES footprints in a 700 km wide Tropical Rainfall Measuring Mission (TRMM) swath, each footprint that meets the selection criteria is marked as part of a cloud object. These "seed points" are grown using the algorithm described in Wielicki and Welch (1986). Only footprints that are adjacent and that meet the selection criteria of a single cloud type can be joined in a cloud object. By adjacent, we mean CERES footprints that are next to each other along the scanning direction, or perpendicular to it. Cloud objects are uniquely determined when they share no adjacent CERES footprints. Cloud objects that grow to an equivalent diameter of less than 100 km, approximately 75 footprints, are ignored in the present analysis to limit data noise. A constant value of 100 km^2 is used for the area of each CERES footprint to calculate the cloud object equivalent diameter. This can cause one-sigma noise in cloud object diameter of roughly 20% since the footprints have variable sizes and shapes. Further details can be found in Xu et al. (2005).

The selection criteria for the tropical deep convective cloud-object type are composed of both cloud top height and τ because we are interested in thick, upper tropospheric anvils and cumulonimbus towers in the tropics. The cloud top height must be greater than 10 km and τ must be greater than 10. The cloud fraction of the footprint must be 100%. Furthermore, all footprints must be located within the Pacific Ocean between 25° S and 25° N.

The selection criteria for boundary-layer cloud-object types are composed of both cloud-top height and cloud fraction. The cloud-top height must be less than 3 km, which is sufficiently high for such clouds without an overlapping high cloud above. The cloud fraction of the footprint must be between 99-100% to be stratus, 40-99% to be stratocumulus and 10-40% to be cumulus. After a cloud object is identified, each footprint is checked to screen out any ice cloud footprint so that only water clouds are included in the data. The threshold of 40% for separating cumulus and stratocumulus clouds is arbitrary, but the lower limit of 10% for cumulus clouds is designed to eliminate uncertainties associated with satellite imager measurements. The selection criteria used in this study are adequate for categorizing the three boundary-layer cloud types seen by ground-based observers, compared to the classification by the International Satellite Cloud Climatology Project (ISCCP; Rossow and Schiffer 1991, 1999). However, additional information such as imager-pixel variabilities would be needed to more rigorously categorize these cloud types seen by ground-based observers. This step was not taken because the present study is not aimed at comparing satellite data with ground-based observations.

3. LINKING CLOUD OBJECTS TO CLIMATE SENSIVITITY

How can an ensemble of cloud objects, which is represented by collections of distinct weather, be linked to climate sensitivity? Based upon linear systems analysis, Schlesinger (1985) defined climate feedbacks including cloud-climate feedbacks in terms of partial derivatives which represent the rates of response of internal variables to changes in external forcings. The feedback strength is decomposed into individual components by assuming that the feedbacks are both independent of each other and linear in nature. Obviously, nonlinearities inherent in cloud-radiation processes distort the analyzed feedbacks in this linear analysis framework. The cloud object approach has the potential to greatly simplify the understanding of cloud-climate feedback processes because the data are not composite averages of very different types of cloud systems. The changes in the feedback strengths are then a combination of the changes in the frequency of occurrence of each individual cloud-system type and the changes in cloud-physical and radiative properties of the same cloud-system type. This is analogous to the separation of cloud property changes into dynamic and thermodynamic components proposed by Bony et al. (2004).

A key step to understand climate sensitivity with cloud object data is to match atmospheric states with observed cloud objects temporally and spatially. Since atmospheric state data from meteorological data assimilations are normally available every six hour, the gap in time matching is usually less than three hours. In matching the location of the cloud object, a rectangular box (latitude x longitude) is drawn to cover the four outermost corner footprints of the cloud object based upon the minimum and maximum latitudes and longitudes of the observed cloud object. That is, parts of the environment surrounding a cloud object are included. Although the ability of an adequate matching between cloud objects and atmospheric states is highly dependent upon the data assimilation system that produces the atmospheric state data, the long-lasting and large-size cloud systems are generally expected to be matched well while the short-

lived and small-size cloud objects are not. This is another reason why cloud objects with equivalent diameters less than 100 km are ignored in the present analysis.

The next step is to categorize large ensembles of cloud objects according to the matched atmospheric states or specific climatic conditions, for example, according to SSTs. Both the changes in the frequency of occurrence and summary histograms with respect to a specific atmospheric-state parameter are examined to derive the total changes in cloud physical and radiative properties. If the summary histograms are not sensitively dependent upon the atmospheric-state parameter, the total changes in cloud properties can be solely determined by changes in the frequency of occurrence of cloud objects. Observed cloud objects are also categorized according to geographic regions. The differences in the summary histograms are also examined to find out the causes for the differences. An example of this will be shown for boundary-layer cloud object types.

4. RESULTS

Table 1 shows the number of tropical deep-convective cloud objects (or the frequency of occurrence) in the Pacific during January-August 1998. The numbers of cloud objects are obtained for five precession cycles and two cloud-object size categories. Each precession cycle of the TRMM satellite is 46 days long. A precession cycle gives a complete sampling of the diurnal cycle at a given location. The cloud-object size category is defined in terms of the equivalent diameters of cloud objects. It appears that the size category with equivalent diameters greater than 100 km has roughly the same number of cloud objects for the five precession cycles(± 12 %). But the large size category with equivalent diameter greater than 300 km has a higher number of cloud objects at the beginning of the January-August period, corresponding to the peak phase of the 1997/1998 El Niño. This suggests that higher SSTs are preferred by larger cloud objects in the Tropics. As expected, relatively fewer numbers of large-size cloud objects were observed during the April-May and June-July cycles as the El Niño dissipated.

Table 1: Number of observed cloud objects during the five precession cycles for two cloud object size categories. The cloud object size is in terms of its equivalent diameter.

Equivalent diameter	Jan. - Feb.	Mar. - Apr.	Apr. - May	June - Jul.	Jul. - Aug.
> 100 km	411	419	362	375	454
> 300 km	121	83	82	82	91

Figure 1 shows summary histograms of four selected parameters for the five precession cycles

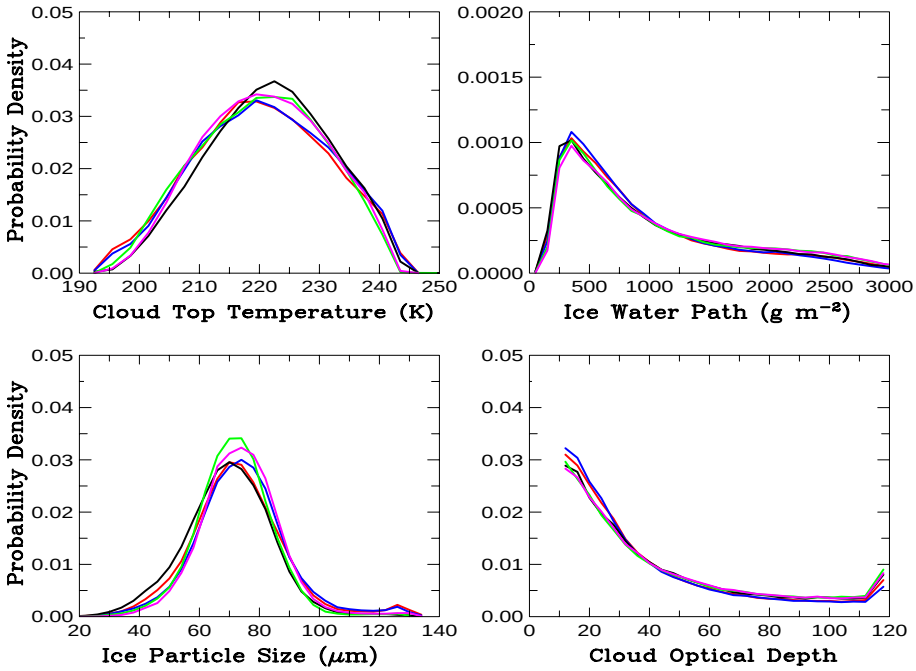

Fig. 1: Summary histograms of cloud top temperature, ice water path, ice particle size and cloud optical depth for large-size (>300 km) cloud objects categorized by satellite precession cycles.

of the large-size (> 300 km) cloud object category. The differences in the histograms among the precession cycles are rather small. They can be quantified by a bootstrap method (Efron and Tibshirani 1993). The details of this testing procedure can be found in Xu (2006). Briefly, the differences in pdfs are measured by a root-mean-square method for two pdfs of the same parameter, which is called the Euclidean distance or L2. This pdf distance measure is defined as

$$\mathrm{L2} = \left\{ \sum_{i=1}^{N} [f(x_i)\Delta x_i - g(x_i)\Delta x_i]^2 \right\}^{1/2},$$

where f and g are two pdfs, with a total of N bins where the ith bin is located at x_i. The bin width is denoted by Δx_i. The frequency of occurrence is normalized by the bin width. That is, f and g satisfy $\sum_{i=1}^{N} f(x_i)\Delta x_i = \sum_{i=1}^{N} g(x_i)\Delta x_i = 1$. The bin width Δx_i is uniform for the pdfs examined here.

The null hypothesis for the bootstrap procedure is that all cloud objects came from the same population for a particular parameter of the measurements, which allows the merging of two cloud-object populations for bootstrap resampling. That is, the choice of which cloud objects were from population A and which were from population B was equivalent to a random choice from the merged data set. Therefore, the distance between the histograms for the "true" ordering is essentially a random number picked from the sampling distribution of the bootstrap distances.

This resampling procedure is repeated M (M is chosen to be 9999 times) time to generate a statistical distribution of the test statistic (L2). For each time, the bootstrap distance value is compared to the value from the true arrangement of cloud objects, i.e. two separate sets or categories of cloud objects. If the bootstrap value of the test statistic of the particular parameter is greater than the observed value of the test statistic in less than 5% of a total calculation of M times, the two sets of cloud objects are deemed to be statistically different for this particular parameter. That is, the threshold p-value is chosen to be 0.05, which means that there is 95% confidence that the two pdfs are significantly different. When the p-value is less than 0.05, there is more than 95% confidence that the two summary histograms are not formed from a statistically similar cloud-object population. In other word, these two pdfs are different.

For the pdfs shown in Fig. 1, the p values between two precession cycles for cloud top temperature are all greater than 0.05 (Xu et al. 2006a). This result suggests that the fixed anvil temperature hypothesis of Hartmann and Larson (2002) is basically supported by the cloud object data despite the large changes of SSTs (not shown).

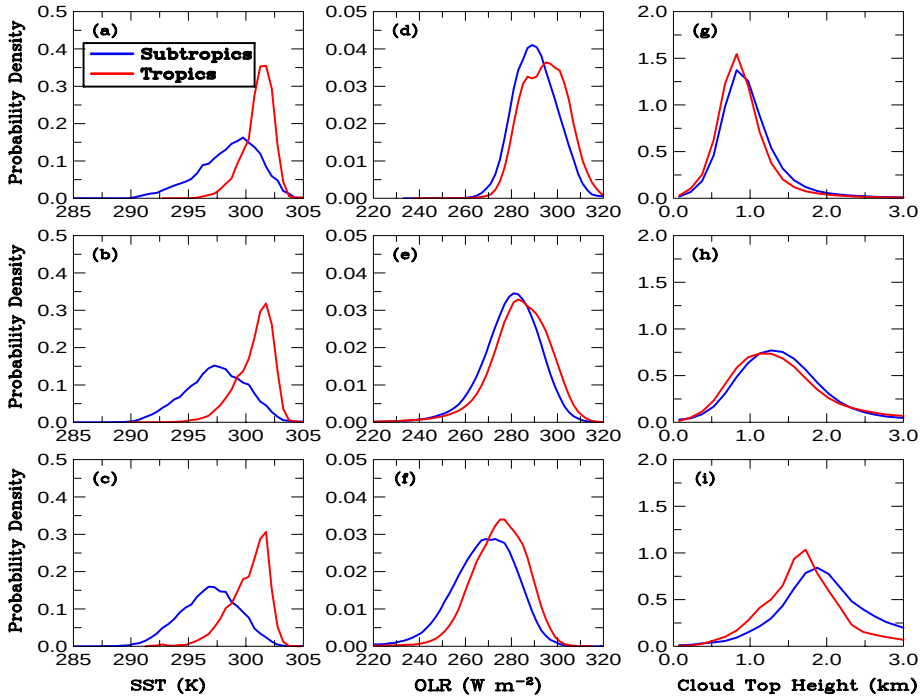

Fig. 2: Summary histograms of SST, outgoing longwave radiation and cloud top height for tropical (red) and subtropical (blue) cumulus (top panels), stratocumulus (middle) and stratus (bottom) cloud objects.

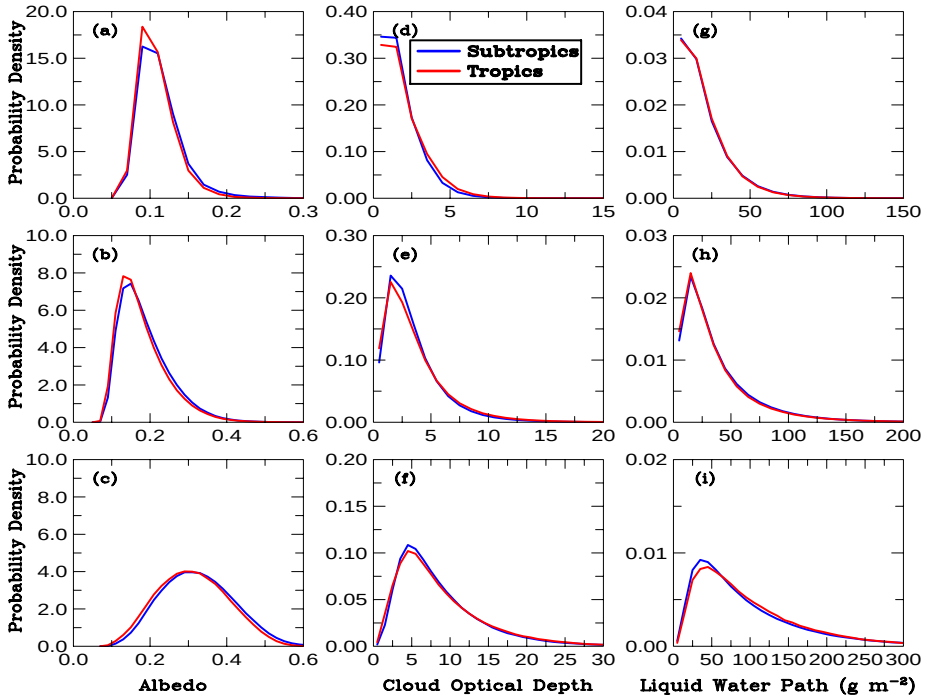

Fig. 3: Same as Fig. 2 except for TOA albedo, cloud optical depth and liquid water path.

Histograms of other parameters given in Fig. 1 show large differences among a few precession cycles, especially between the first and last precession cycles (red vs. pink curves). Further detailed discussion can be found in Xu et al. (2006a).

Another example of the cloud-object analyses is shown for boundary-layer cloud object types, which contrasts the tropical and subtropical regions. There are significant differences in all statistical properties among the three cloud-object types and between the tropics and subtropics (Figs. 2 and 3). A detailed explanation for the differences among the cloud-object types is given in Xu et al. (2005). All cloud objects with equivalent diameters between 75 and 300 km are included in producing the summary histograms shown in Figs. 2 and 3 using between 0.5 and 1.7 million footprints.

Each of the three cloud object types exhibits small differences in cloud optical depth, liquid water path, TOA albedo, moderate differences in cloud-top height, but large differences in cloud-top temperature (not shown) and OLR between the tropics and subtropics. The latter two properties are tightly related to the differences in the SST distributions between the tropics and subtropics. It should be pointed out that these differences between the tropics and subtropics are smaller than those among the cloud object types shown in Fig. 2 and 3. These results suggest that SST distributions strongly influence cloud macrophysical properties, but only weakly influence cloud microphysical properties and albedo for each cloud object type. The latter distributions are robustly determined by distinct boundary-layer dynamics and structures of each cloud object type.

5. CONCLUSIONS

This study has presented a new methodology for studying cloud feedback and climate sensitivity using the satellite cloud-object data. The cloud object analysis approach links cloud organization to climate sensitivity via matching the observed cloud objects with atmospheric state data in time and space. Satellite footprint data have been analyzed to produce large ensembles of cloud objects for different size categories, SSTs or climate regimes. In this study, the statistics of the observed cloud objects are analyzed to understand the cloud feedbacks, in particular, to validate the fixed anvil temperature hypothesis of Hartmann and Larson (2002) and to understand the differences in the statistical cloud properties between the tropical and subtropical boundary-layer cloud object types.

Acknowledgments: This research has been supported by NASA EOS Interdisciplinary Study Program and Cloud Modeling and Analysis Initiative managed by Dr. Donald Anderson.

REFERENCES

Bony, S., J.-L. Dufresne, H. Le Treut, J.-J. Morcrette and C. Senior, 2004: On dynamic and thermodynamic components of cloud changes. *Climate Dyn.,* **22,** 71-86. doi: 10.1007/s00382-003-0369-6.

Hartmann, D. L., and K. Larson, 2002: An important constraint on tropical cloud-climate feedback. *Geophs. Res. Lett., doi:1029/ 2002GL015835.*

Rossow, W. B., and R. A. Schiffer, 1991: ISCCP cloud data products. *Bull. Amer. Meteor. Soc.*, **72**, 2-20.

Rossow, W. B., and R. A. Schiffer, 1999: Advances in understanding clouds from ISCCP. *Bull. Amer. Meteor. Soc.*, **80**, 2261-2287.

Schlesinger, M. E., 1985: Feedback analysis of results from energy balance and radiative-convective models. Projecting the Climatic Effects of Increasing Carbon Dioxide, M. C. MacCracken and F. M. Luther, Eds., U.S. Department of Energy, 280–319.

Wielicki, B. A., and R. M. Welch, 1986: Cumulus cloud properties derived using Landsat satellite data. *J. Clim. Appl. Meteor.,* **25,** 261-276.

Wielicki, B. A., B. R. Barkstrom, E. F. Harrison, R. B. Lee III, G. L. Smith, and J. E. Cooper, 1996: Clouds and the Earth's Radiant Energy System (CERES): An Earth Observing System Experiment. *Bull. Amer. Meteor. Soc.*, 77, 853-868.

Xu, K.-M., 2006: Applying the bootstrap method for statistical significance test of differences between histograms. *Mon. Wea. Rev.*, **134,** 1442–1453.

Xu, K.-M., T. Wong, B. A. Wielicki, L. Parker, and Z. A. Eitzen, 2005: Statistical analyses of satellite cloud object data from CERES. Part I: Methodology and preliminary results of 1998 El Niño/ 2000 La Niña. *J. Climate,* **18,** 2497-2514.

Xu, K.-M., T. Wong, B. A. Wielicki, L. Parker, B. Lin, Z. A. Eitzen, and M. Branson, 2006a: Statistical analyses of satellite cloud object data from CERES. Part II: Tropical convective cloud objects during 1998 El Niño and evidence for supporting the fixed anvil temperature hypothesis. *J. Climate,* in press [Available from http://asd-www.larc.nasa.gov/~tak/wong/f21m.pdf].

Xu, K.-M., T. Wong, B. A. Wielicki, L. Parker, 2006b: Statistical analyses of satellite cloud object data from CERES. Part IV: Boundary-layer cloud objects during 1998 El Niño. *J. Climate* (submitted).